



## ORIGINAL ARTICLE

# Removal of Pb(II) from aqueous solutions by using steelmaking industry wastes: Effect of blast furnace dust's chemical composition



Ma. de Jesús Soria-Aguilar<sup>a</sup>, Antonia Martínez-Luévanos<sup>b</sup>,  
Marco Antonio Sánchez-Castillo<sup>c,\*</sup>, Francisco Raul Carrillo-Pedroza<sup>a,\*</sup>,  
Norman Toro<sup>d</sup>, Victor Manuel Narváez-García<sup>b</sup>

<sup>a</sup> Facultad de Metalurgia, Universidad Autónoma de Coahuila, Carretera 57 Km 5, 25710 Monclova, Coahuila, Mexico

<sup>b</sup> Facultad de Ciencias Químicas, Universidad Autónoma de Coahuila, Ing. J. Cárdenas Valdez S/N, República, 25280 Saltillo, Coahuila, Mexico

<sup>c</sup> Facultad de Ciencias Químicas, Universidad Autónoma de San Luis Potosí, Manuel Nava 6, San Luis Potosí, S.L.P. 78210, Mexico

<sup>d</sup> Departamento de Ingeniería Metalúrgica y Minas, Universidad Católica del Norte, Av. Angamos 0610, Antofagasta, Chile

Received 2 November 2020; accepted 4 February 2021

Available online 17 February 2021

## KEYWORDS

Metallurgical residues;  
Steelmaking wastes valorisation;  
Pb(II) removal;  
Sustainable processes.

**Abstract** Slags, sludges, and dust from steelmaking industries have been probed as adsorbents for Pb(II) removal from synthetic water solutions, and these residues have showed good potential in the treatment of industrial effluents contaminated with this heavy metal. Adsorption and precipitation of Pb(II) have been postulated as the main mechanisms to remove Pb(II) from aqueous solutions by using steelmaking residues. The significant effect of pH on Pb(II) removal has been well studied but few studies explicitly address the effect of chemical and mineralogical composition of steelmaking residues and a better understanding of this key parameter is still needed for full elucidation and optimization of the Pb(II) removal process. In this study, samples obtained from different sections of a dust collector system (BFD) in a steelmaking factory, were used to evaluate the effect of BFD sample's chemical composition on the removal of Pb(II) from synthetic aqueous solution. BFD samples were characterized to determine their chemical composition, particle size distribution and isoionic point. Equilibrium and transient experiments of Pb(II) removal from aqueous solutions were conducted at 25 °C and initial pH = 5.0. Results showed that CaO and MgO, as well as metallic Fe and FeO had a positive linear effect on BFD samples Pb(II) adsorption capacity. Pb(II) removal process may take place by ion exchange with CaO and MgO, and by precipitation

\* Corresponding authors.

E-mail addresses: [masanchez@uaslp.mx](mailto:masanchez@uaslp.mx) (M.A. Sánchez-Castillo), [raul.carrillo@uadec.edu.mx](mailto:raul.carrillo@uadec.edu.mx) (F.R. Carrillo-Pedroza).

Peer review under responsibility of King Saud University.



Production and hosting by Elsevier

on the surface of metallic Fe and FeO. MgO and FeO promoted the Pb(II) removal in lesser extent than CaO and metallic Fe, respectively, because the surface ion exchange with MgO and FeO are less thermodynamic favourable and their lower composition in the sample. Bimolecular ion exchange process between Pb(II) ions and Ca and Fe species was supported by results from equilibrium and transient adsorption studies. Results of this work clearly showed that removal of Pb(II) from aqueous solutions is a strong function of the chemical composition of BFD samples and it provided further insight to promote the valorisation and optimization of steelmaking residues as heavy-metal adsorbents.

© 2021 The Authors. Published by Elsevier B.V. on behalf of King Saud University. This is an open access article under the CC BY-NC-ND license (<http://creativecommons.org/licenses/by-nc-nd/4.0/>).

## 1. Introduction

Lead is listed as one of the top 10 chemicals of public health concern by the World Health Organization Chemical Safety Agenda (PAHO, 2020). Disposal of untreated wastewater effluents on processing industries such as acid battery manufacturing, metal plating and finishing, tetraethyl lead manufacturing, ceramic and glass industries and environmental clean-up services is one of the major sources of water pollution by lead (Vijayakumar et al., 2012; Arbabi et al., 2015; Vu et al., 2019). The permissible concentration limit for Pb(II) in industrial wastewater effluents, set by the Environmental Protection Agency (EPA), is 0.05 mg/L; however, in many wastewater effluents Pb(II) concentration is the range of 200–500 mg/L. For this reason, it is imperative to reduce Pb(II) concentration to a level of 0.05–0.10 mg/L before the wastewater effluent be discharged to municipal sewage systems (Arbabi et al., 2015; WHO, 2020).

Several methods have been used to remove Pb from wastewater effluents, including chemical precipitation, electrochemical reduction, ion exchange, reverse osmosis, membrane separation, and adsorption (Arbabi et al., 2015; Bădescu et al., 2018). These technologies have proven to be effective for Pb removal, but they also exhibit some disadvantages such as continuous input of chemicals, high cost, toxic sludge generation or incomplete Pb removal. To date, adsorption technology still stands as a suitable alternative for the treatment of heavy metal polluted wastewaters because of recent developments of more selective adsorbents with increased adsorption capacity and, also, because the technology is simple and it may save operating costs if an appropriate adsorbent regeneration process is developed (Al-Asheh et al., 2000; Zahra and Pak, 2012).

Several smart materials have recently been explored as highly efficient adsorbents for removal of Pb(II) ions from aqueous solutions. Different types of nanoparticles and nanocomposites (Fe, Zn, SiO<sub>2</sub>, Ti, SiC, Mo, Ce, graphene) have been reported for the removal of Pb(II) from aqueous media, but technological and economic issues still limit their practical applications (Ata et al., 2018; Alghamdi et al., 2019; Lucaci et al., 2019). For this reason, there is an ongoing effort to improve the adsorption capacity and selectivity of conventional low-cost adsorbents including activated carbon, bentonite, chitosan and iron oxides such as magnetite, hematite and maghemite (naturals or synthesized), which are capable of adsorbing lead and other heavy metal ions from aqueous solutions (Olowoyo and Garuba, 2012; Roy and Bhattacharya, 2012; Zhu et al., 2012; Xiong et al., 2015; Hosseinzadeh et al., 2016). In addition, development of low-cost adsorbents based

on the use of industrial solid wastes, such as red mud, fly ash, dusts and slags also have also been studied as potential Pb(II) adsorbents (Ghaedi and Mosallanejad, 2013; Chung et al., 2016; Juned et al., 2016; Soliman and Moustafa, 2020). This approach of reuse industrial residues than may cause health and environmental risks is particularly useful in the current context of circular economy, as it has beneficial impacts in terms of developing sustainable industrial processes.

In particular, slags, sludges, and dusts from steelmaking industry have been investigated as promising feedstock for several applications. A large availability of these industrial residues is foreseen given the fact that steelmaking industry steel has sustained a significant average growth rate over the last decade and also because steelmaking residues amount up for 1–4% of hot metal production (Jalkanen et al., 2005; Andersson et al., 2017; Naidu et al., 2020). Given the fact that it is impractical to recycle steelmaking residues due to operational difficulties in the blast furnace (Sarkar and Mazumder, 2015), they are being reused in an increasing number of innovative applications such as construction materials, soil enrichment and treatment, environmental remediation (including waste stabilization, carbon capture and storage and mitigation on landfill emissions) and water treatment of industrial effluents. Very importantly, the beneficial impact of steelmaking residues in a given application is highly dependent on their physical and chemical properties (Fisher and Barron, 2019; Naidu et al., 2020). Blast furnace (BF) and Basic Oxygen Furnace (BOF) dusts and slags have been used to remove heavy metals cations, anions or organic toxic compounds from synthetic water solutions and from polluted water effluents (Huy et al., 2020; Kennedy and Arias-Paić, 2020; Naidu et al., 2020; Vu et al., 2021). In particular, literature shows that BF and BOF dusts and slags are low-cost adsorbents to remove Pb(II) ions from aqueous solutions over a wide range of experimental conditions (Srivastava et al., 1997; Lopez-Delgado et al., 1998; Bhatnagar and Jain, 2006; Liu et al., 2010; Chung et al., 2016; Bouabidi et al., 2018; Yang et al., 2019; Zhan et al., 2019; Huy et al., 2020; Mercado-Borraro et al., 2020; Kim et al., 2021). As it could be expected, the efficiency of heavy metals removal from aqueous solutions by using steelmaking residues is determined by the physical and chemical properties of the residues and the set of experimental conditions during the metal removal process. The initial metal concentration, temperature, pH and ionic strength of the metal aqueous solution determine the nature and distribution of the ionic species in solution. In the other hand, the physical properties, such as surface area and porosity, regulate the accessibility of the ionic species to the adsorption or active

sites, and the surface chemical properties play a major role to control the nature, the equilibrium and the kinetics of the surface processes taking place to remove the metal ions from the aqueous solution (Yiacoumi and Tien, 1995; Cooney, 1998). Adsorption and precipitation of Pb(II) have been postulated as the main mechanisms to remove Pb(II) from aqueous solutions by using steelmaking residues. It has been reported that pH of Pb(II) solution plays a major role to determine extent of each Pb(II) removal mechanism (Nassar, 2010; Yang et al., 2019; Huy et al, 2020; Soliman and Moustafa, 2020; Kim et al, 2021). However, very few studies explicitly address the effect of chemical composition of steelmaking residues in Pb (II) removal from aqueous solutions (Lopez-Delgado et al., 1998; Nilforoushan and Otroj, 2008), and a better understanding of this key parameter is still needed for full elucidation of the Pb(II) removal process. This information will facilitate the valorisation of steelmaking residues as Pb(II) adsorbents or catalysts in the remediation of Pb(II) polluted aqueous effluents.

In this study, four dust samples collected in different section of a blast furnace (BFD samples), were used to determine the effect of BFD's chemical composition in the removal capacity of Pb(II) from aqueous solutions. To this purpose, composition of BFD samples was characterized by atomic adsorption spectroscopy and X-Ray fluorescence; the particle size and the isoionic point of BFD samples were also determined. Experimental test of Pb(II) removal capacity from aqueous solutions were conducted in a batch system at 25 °C and pH = 5.0. The effect of BFD's chemical composition in Pb(II) removal capacity, as well as in the Pb(II) removal mechanism under the conditions of the study were rationalized based on previous findings in the literature.

## 2. Experimental

### 2.1. BFD characterization

Four BFD samples were collected from a dust collector system installed in a major integrated steelmaking plant in Mexico. As schematically shown in Fig. 1, sample A (SA) was collected from the dust catcher, sample B (SB) from the dust cyclone, sample C (SC) from the wet scrubber, and sample D (SD) was obtained from the sludge dam. The samples were only shredded (to break up lumps or agglomerates) and dried at 105 °C for 24 h, to obtain representative samples.

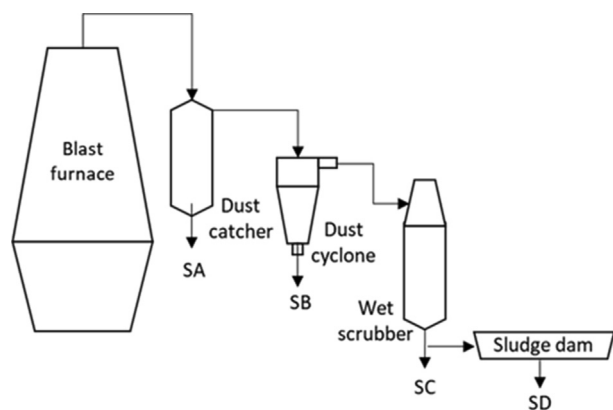


**Fig. 1** Schematic representation of a blast furnace dust collector system.

Chemical analysis of the BFD samples was carried out by atomic absorption spectroscopy (AAS) using a Thermo Electron Solaar S4 spectrophotometer. Quantification of each cation was performed using the corresponding ASTM method. For Ca, K and Na (reported as CaO, K<sub>2</sub>O and Na<sub>2</sub>O, respectively), a 0.2% w/v Cl<sub>3</sub>La solution was added to prevent signal reduction caused by aluminium and a 0.1% w/v CsCl solution was added as an ionization buffer. Mg and Al (reported as MgO and Al<sub>2</sub>O<sub>3</sub>) were measured under more oxidative conditions using a N<sub>2</sub>O/acetylene gas mixture. SiO<sub>2</sub> retained in the solid was determined by gravimetry (by oxidation with HClO<sub>4</sub>). Sulphur and total carbon were determined by using a LECO CS-244 analyser.

Complementary, chemical analyses were also performed by using X-Ray fluorescence (XRF) using a Bruker AXS S4 PIONEER spectrophotometer. Iron phases composition were determined by X-ray diffraction (XRD) using a Bruker D8 diffractometer equipped with monochromatized Cu<sub>Kα</sub> radiation (generator tension = 40 kV, current = 30 mA). XRD pattern was recorded from (2θ) 5 to 70°, with step size of 0.02° and a counting time of 0.4 s per step. Rietveld method was used to quantify iron phases in BFD samples.

Particle size distributions for BFD samples were determined by using Tyler sieves. In addition, the isoionic point (IIP) of BFD slurries was determined by potentiometric titration. Experiments were performed using 1 g of BFD and 160 mL of an ionic strength regulated solution (NaNO<sub>3</sub> = 10<sup>-3</sup> M). The evolution of the slurry pH, initially acid or alkaline, was measured during titration with HCl or NaOH until the slurry pH remained constant, as an indication that an equilibrium condition had been reached.

### 2.2. Pb(II) removal tests

Experiments to evaluate the effect of BFD samples chemical composition in the removal of Pb(II) cations were carried out with synthetic Pb(II) aqueous solutions, which were prepared by using lead nitrate (Aldrich, chemical grade) and distilled water. Experiments were conducted in a 200 mL batch reactor (borosilicate conical bottles) with different Pb(II) concentration (obtained by dissolution from a stock solution with initial Pb(II) concentration of 538 mg/L) and initial pH = 5, which was fixed by using HNO<sub>3</sub> analytical grade reactive. This initial pH was selected to avoid the precipitation of Pb(II) as Pb(OH)<sub>2</sub>, which occurs around pH = 5.5. In each experiment, a given load of BFD (1 g) was added to 100 mL of a Pb(II) aqueous solution; then, the adsorption process took place at atmospheric pressure, 25 °C and under stirring condition at 300 rpm, for up to 6 h. Afterwards, the resulting suspension was filtered. The concentration of lead in the aqueous solution was quantified before and after the adsorption test by atomic absorption spectroscopy (AAS, Perkin Elmer 3100), using an appropriate lead calibration curve. The effects of contact time, BFD load and lead initial concentration on the Pb(II) removal process were also studied in similar sets of experiments.

## 3. Results and discussion

### 3.1. BFD characterization

Table 1 shows the chemical composition of the BFD samples used in this study. Iron species were the major component in

**Table 1** Chemical composition (%) of SA, SB, SC and SD samples.

Sample	Fe	CaO	C	SiO <sub>2</sub>	Al <sub>2</sub> O <sub>3</sub>	MgO	Zn
SA	48.08	6.01	16.20	6.57	0.94	1.44	0.25
SB	35.78	14.22	32.80	8.72	0.91	1.17	0.28
SC	41.16	26.93	6.00	4.33	0.91	4.39	0.44
SD	46.19	24.45	4.39	3.45	0.50	3.74	1.56

**Table 2** Iron phases distribution (%) in SA, SB, SC and SD.

Sample	Fe <sub>2</sub> O <sub>3</sub>	Fe <sub>3</sub> O <sub>4</sub>	FeO	Fe <sup>0</sup>	Fe <sub>2</sub> ZnO <sub>4</sub>	Sum of Fe
SA	15.04	12.53	11.03	9.02	0.45	48.08
SB	13.77	11.80	7.87	1.97	0.37	35.78
SC	2.13	6.40	14.92	17.06	0.66	41.16
SD	1.42	7.05	16.46	18.82	2.44	46.19

all BFD samples. In addition, a significant amount of C was also measured in all samples. The higher C content was found in catcher's sample (SA) and cyclone's sample (SB) (16.2 and 36.8%, respectively). Basic oxides such as CaO, SiO<sub>2</sub> and MgO were also found. Wet scrubber sample (SC) and sludge dam sample (SD) showed the higher CaO (26.93 and 24.45%, respectively) and MgO (4.39 and 3.74%) content. Residual quantities of Zn (0.25–1.6%) and Al<sub>2</sub>O<sub>3</sub> (less than 1%) were also quantified in all samples. The presence of iron oxides and basic oxides have been reported in the literature as active sites or species to promote the removal of Pb(II) from aqueous solutions (Ugwu and Igbokwe, 2019).

In closer detail, Table 2 includes the specific iron phases found in the BFD samples. In addition, phase percentages were calculated based on the amount of total iron distributed in each phase. Clearly, all BFD samples contained the following iron phases: hematite (Fe<sub>2</sub>O<sub>3</sub>), magnetite (Fe<sub>3</sub>O<sub>4</sub>), wustite (FeO) and metallic or zero-valence iron (Fe<sup>0</sup>). Smaller amounts of franklinite (Fe<sub>2</sub>ZnO<sub>4</sub>) were also found in BFD samples, in agreement with the chemical analysis that showed the presence of a residual amount of Zn. Iron phase distribution was clearly different in the BFD samples. For SA and SB, iron was predominantly found as hematite and magnetite, followed by wustite and metallic iron. In the other hand, for SC and SD the main iron phases were metallic iron and wustite. The main difference in the composition of SC and SD was the franklinite content as a result that SD was collected from the sludge dam, which is used in the steelmaking factory to collect dusts from other steelmaking operations.

Table 3 includes the particle size of BFD samples, given as D<sub>90</sub> (90% of the particles pass or have a size less than the corresponding mesh). SA had a D<sub>90</sub> = 150 μm indicating that

**Table 3** Particle size (D<sub>90</sub>) and isoionic point of SA, SB, SC and SD samples.

Sample	Particle size, D <sub>90</sub> , μm	Isoionic point, pH <sub>IIP</sub>
SA	150	5.0
SB	75	6.4
SC	20	5.7
SD	15	5.5

particles with a D less than 150 μm were collected by the dust catcher. According to chemical and phase analysis, the particles that are dragged and trapped by the catcher have undergone little decomposition or reduction (or oxidation in the case of coal). The particles with smaller size that were not collected in the catcher, went to the dust cyclone, which collected particles (SB) with a D<sub>90</sub> = 75 μm, but larger than 20 μm. The dust trapped by the cyclone also had a low degree of reduction and high carbon content. In a subsequent stage, smaller particles still dragged by the gases were trapped in the last collector equipment, the wet scrubber. The characteristic size of these particles (SC) was D<sub>90</sub> = 20 μm. In this stage, particles had suffered the greatest reduction (and calcination in the case of limestone). The dust discharged from the wet scrubber was deposited on a sludge dam, which also contain dusts from others BF and BOF; the particle size of a sample taken from the sludge dam (SD) was D<sub>90</sub> = 15 μm. In the other hand, Table 3 also includes the isoionic points (IIP) of the BFD samples, which varied in a relatively close range, from pH = 5–10 to 6.4, suggesting a slightly surface acid character. It should be noticed that the IIP of BFD samples was in close agreement with the IIP reported in the literature for similar industrial residues, and also for the IIP of pure hematite and magnetite species (Rezaei and Vione, 2018; Kosmulski, 2020). The IIP of BFD samples is helpful to elucidate the removal mechanism of Pb(II) from aqueous solutions.

### 3.2. Effect of the chemical composition and particle size in Pb (II) removal from aqueous solutions

The effect of chemical composition of BFD samples on Pb(II) removal from aqueous solutions was determined by comparing the maximum Pb(II) removal percentage by SA, SB, SC and SD, at 25 °C, initial pH = 5. To this purpose, for each sample, a series of experiments were conducted by varying the initial Pb(II) concentration, C<sub>0</sub>, from 54 to 538 mg/L and using a sample load of 1 g. The corresponding equilibrium Pb(II) concentration in the aqueous solution, C<sub>e</sub> (mg/L), was obtained when Pb(II) concentration did not change over time. Pb(II) removal percentage (Pb(II)<sub>removal</sub>) was calculated by using the following equation:

$$Pb(II)_{removal}, \% = \frac{C_e - C_0}{C_0} \times 100 \quad (1)$$

Fig. 2 shows Pb(II)<sub>removal</sub> as a function of C<sub>e</sub> for the BFD samples used in this study. The C<sub>e</sub> corresponding to the maximum Pb(II)<sub>removal</sub> reached in each sample (C<sub>e, max</sub>) was used to calculate the maximum Pb(II) adsorption capacity per gram of adsorbent, Q<sub>e</sub> (mg/g), by using the following equation:

$$Q_e = \frac{(C_0 - C_{e, max})V}{W} \quad (2)$$

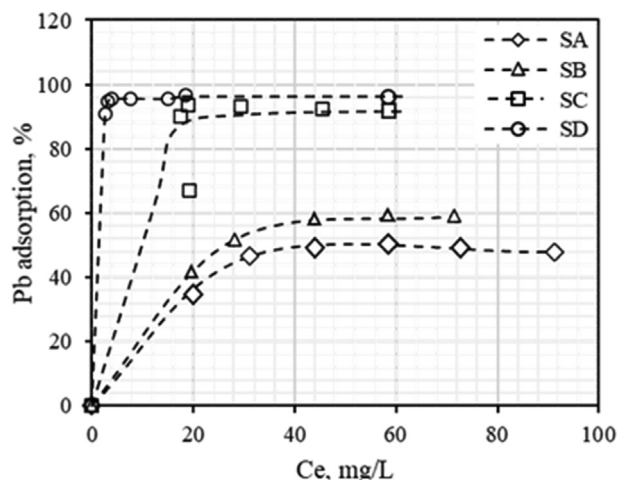
where V is the volume of solution (100 mL) and W is the total mass of adsorbent (1 g).

The main results of Fig. 2 are summarized in Table 4 includes the values of Pb(II)<sub>removal</sub> and Q<sub>e</sub> for each of sample. Under the conditions used in the study, the maximum Pb(II)<sub>removal</sub> was 43.6, 50.7, 92.9 and 96.1% for the SA, SB, SC and SD samples, respectively. Similarly, the Q<sub>e</sub> value for these samples was 45.1, 59.6, 107.6, and 112.8 mg/g.

In the other hand, Table 5 qualitatively compares the Q<sub>e</sub> values determined for the BFD samples used in this study with

**Table 4** Results of chemical composition and Pb(II) adsorption parameters at Pb(II) concentration = 538 mg/L, 1 g BFD and 25 °C.

BFD	CaO + MgO, %	Iron phases, %	Fe <sup>0</sup> , %	D <sub>90</sub> , μm	pH <sub>IPP</sub>	Pb(II) removal, %	Q <sub>e</sub> , mg/g
SA	7.45	39.05	9.02	150	5.0	43.6	45.1
SB	15.39	33.82	1.97	75	6.4	50.7	59.6
SC	31.32	24.11	17.06	20	5.7	92.9	107.6
SD	28.19	27.37	18.82	15	5.5	96.1	112.8

**Fig. 2** Pb(II)<sub>removal</sub> as a function of C<sub>e</sub> for SA, SB, SC and SD, at 25 °C and initial pH = 5.0.**Table 5** Comparison of Q<sub>e</sub> values obtained for Pb(II) removal from aqueous solutions with various steelmaking residues.

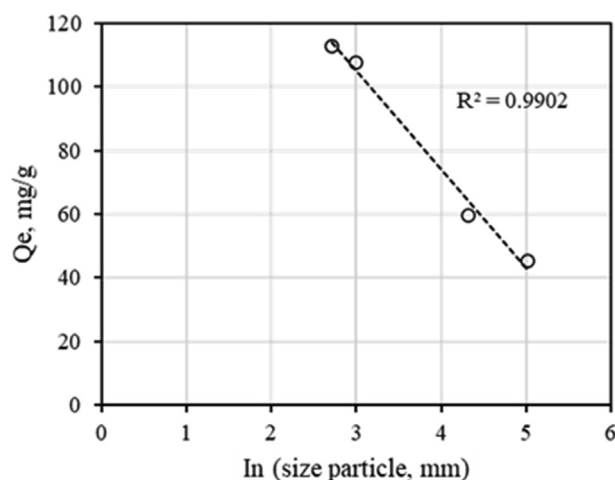
Material	Particle size	Q <sub>e</sub> , mg/g	Reference
Furnace slag	na	4.93	Chung et al., 2016
Cyclone steel dust	~600 nm	39.8	Bouabidi et al., 2018
Ladle furnace steel dust	~600 nm	208.9	Bouabidi et al., 2018
Blast furnace sludge	~40 μm	64.42	Lopez-Delgado et al., 1998
High carbon content sludge	150 μm	55.04	Lopez-Delgado et al., 1998
Steel slag	49–149 μm	6.6	Mercado-Borrayo et al., 2020
Blast furnace slag	150–200 μm	2.27	Srivastava et al., 1997
Blast furnace sludge	na	227	Bhatnagar and Jain, 2006
Blast furnace dust	na	142	Bhatnagar and Jain, 2006
Blast furnace slag	na	25	Bhatnagar and Jain, 2006
Blast furnace SA	150 μm	45.1	This work
Blast furnace SB	75 μm	59.6	This work
Blast furnace SC	20 μm	107.6	This work
Blast furnace SD	15 μm	112.8	This work

na = no available

Q<sub>e</sub> values reported in the literature for the removal of Pb(II) from aqueous solutions by using similar steelmaking residues and similar experimental conditions (temperature = 20–25 °C and pH = 5 and 5.5). It must be noticed that the experimental conditions used in each data set were different and, therefore, the comparison of the maximum Pb(II) removal capacity should only be made in qualitatively basis. Taking into account this fact, SC and SD showed Q<sub>e</sub> of 107.6 and 112.8 mg/g, respectively, which were within the range of Q<sub>e</sub> values reported in Table 5 for residues such as BF sludge and ladle furnace steel dust.

In the condition used in the study, BFD samples particle size varied from D<sub>90</sub> = 150 μm (SA) to D<sub>90</sub> = 15 μm (SD). It was expected that particle size could affect the Q<sub>e</sub> value. In fact, Fig. 3 shows that Q<sub>e</sub> had a linear dependence with the ln of particle size (ln D<sub>90</sub>). Clearly, SD (D<sub>90</sub> = 15 μm) led to a higher Q<sub>e</sub>. These results could be explained in terms that a smaller particle size leads to a larger specific surface area. In this condition, a larger number of adsorption or active sites were available for Pb(II) removal from aqueous solution. This results might also suggest that no internal transport effects were limiting the surface phenomena responsible for Pb(II) removal.

Based on these results, it was evident that, under the conditions used in this study, Pb(II) removal was influenced by the chemical composition of BFD samples. As discussed, each sample had different distribution of their main chemical constituents: iron species (hematite, magnetite, wustite and metallic iron), basic oxides (CaO, SiO<sub>2</sub>, MgO) and carbon species. To elucidate if there was a trend between the chemical composition and Q<sub>e</sub>, Pearson's correlation coefficients were calculated to determine which chemical species had significant

**Fig. 3** Effect of ln particle size (ln D<sub>90</sub>) in Q<sub>e</sub>.

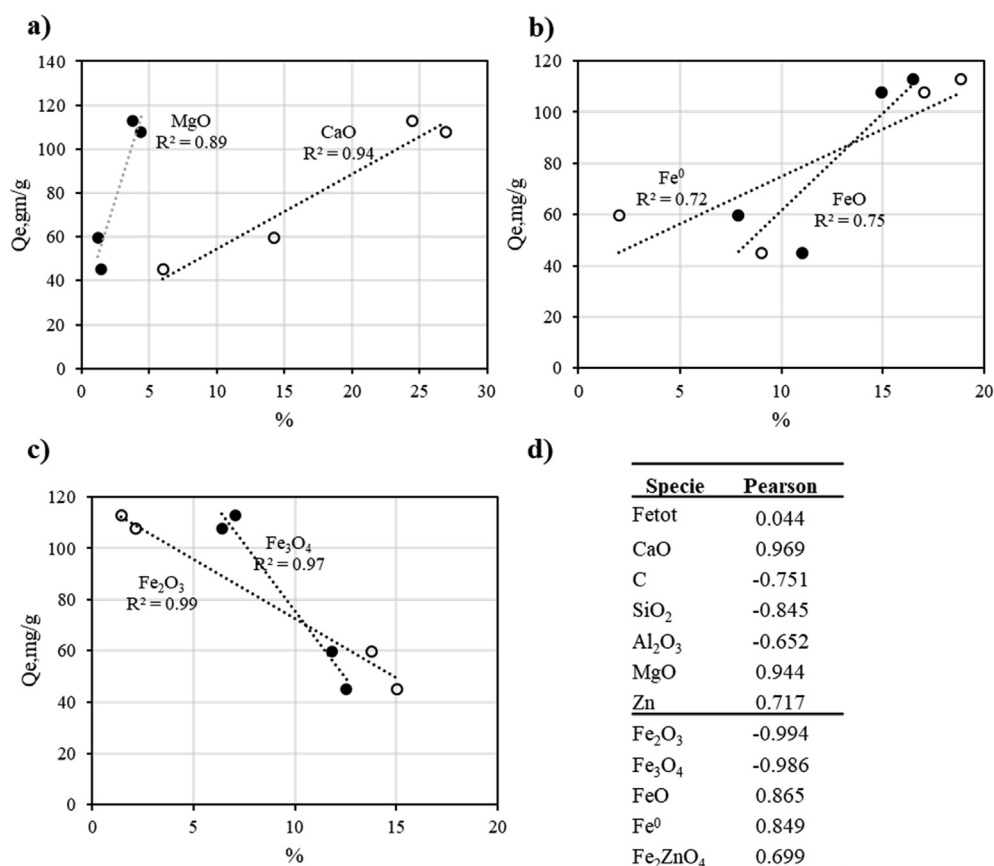


**Fig. 4** Effect of the content of: a) CaO and MgO, b) Fe<sup>0</sup> and FeO, and c) Fe<sub>3</sub>O<sub>4</sub> and Fe<sub>2</sub>O<sub>3</sub> on Q<sub>e</sub>; d) Summary of Pearson's correlation coefficients for the chemical species in BFD samples.

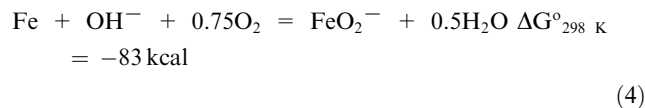
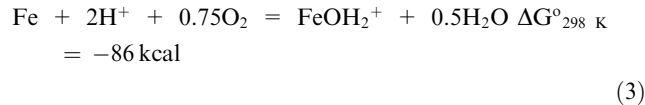
effect on Q<sub>e</sub>. Pearson's correlation coefficient is the covariance of the two variables divided by the product of their standard deviations (Asuero et al., 2006). A correlation value of 0.7 or higher between two variables would indicate that a significant and positive relationship exists between the two (Boslaugh and Watters, 2008). Fig. 4a) shows that Q<sub>e</sub> increased with the content of CaO and MgO. Similarly, Fig. 4b) shows that an increase in metallic iron and wustite enhanced Q<sub>e</sub>. In the other hand, Fig. 4c) indicates that an increasing content of more oxidized iron species (hematite and magnetite) led to a decrease in Q<sub>e</sub>. As a summary, Fig. 4d) includes Pearson's correlation coefficients for a linear association between the chemical phases content in BFD samples and Q<sub>e</sub>. In all cases Pearson's correlation coefficients were higher than 0.72. Positive values suggested a beneficial effect of a given chemical species on Q<sub>e</sub>, and a negative coefficient indicated a detrimental effect of chemical composition on Q<sub>e</sub>. Thus, under the conditions of this study, it could be postulated that Pb(II) removal was enhanced by the content of Fe and FeO, as well as CaO and MgO. Based on the Pearson's correlation coefficients, the basic oxides seem to have a stronger effect on Pb(II) removal. In the other hand, analysis of Pearson's correlation coefficients also suggested that the content of more oxidized iron species such hematite and magnetite, as well as C and SiO<sub>2</sub> had a detrimental effect in Pb(II) removal from aqueous solutions.

With respect to the surface phenomena responsible for Pb(II) removal from aqueous solutions by using steelmaking resi-

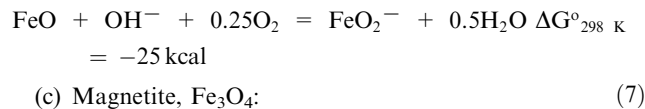
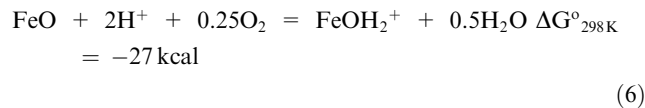
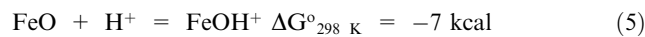
dues, several authors have suggested the occurrence of two competitive processes: Pb(II) adsorption and Pb precipitation. The prevalence and the extent of each surface process has been found highly dependent on the experimental set up: the adsorbent's structure and surface composition as well as the operating conditions: temperature, initial pH, ionic strength, initial Pb(II) concentration, adsorbent load and contact time, among the most relevant parameters (Yang et al., 2019; Huy et al., 2020; Soliman and Moustafa, 2020; Kim et al., 2021). Related to the effect of chemical composition, iron species and basic oxides has been indicated to play a key role in Pb(II) removal from aqueous solutions when using steelmaking residues as adsorbents (Yiacoumi and Tien, 1995). The effect of iron species composition on Pb(II) removal have been related to the number of surface Fe OH<sup>-</sup> groups formed when an iron oxide is immersed in aqueous solution, which favours an adsorption process by electrostatic attraction. In this case, the adsorbent IIP and the ionic species distribution in the aqueous solution are key parameters to determine if such adsorption process is taking place (Cooney, 1998). As it is well known, the IIP determines the adsorbent's surface species that are formed as a function of the solution pH. When an adsorbent is placed in a solution which pH > IIP, the adsorbent will develop positively-charged surface groups. In the other hand if the solution pH > IIP, the adsorbent will develop negatively-charged surface groups. Under these conditions a solution with pH > IIP is preferential to promote the adsorption of positively-charged cations by electrostatic attraction. In

agreement with the chemical composition of the BDF samples used in this study, and based on calculations made with HSC 6.1 (Roine, 2006), iron species may undergo the following protonation and deprotonation surface reactions:

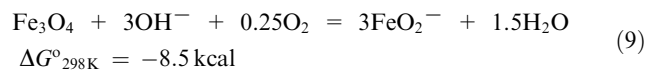
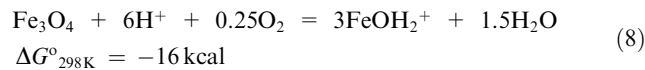
(a) Zero valent iron



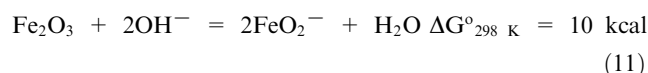
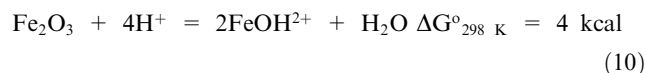
(b) Wustite, FeO



(c) Magnetite, Fe<sub>3</sub>O<sub>4</sub>:



(d) Hematite, Fe<sub>2</sub>O<sub>3</sub>:



As it is reported in the literature, the following reactions may also be taking place as a function of solution pH (Kosmulski, 2020):



As shown in Table 4, the IIP of the BFD samples of this study were in the range of 5.0–6.4. Therefore, when these samples are placed in a solution with pH = 5.0, the formation of

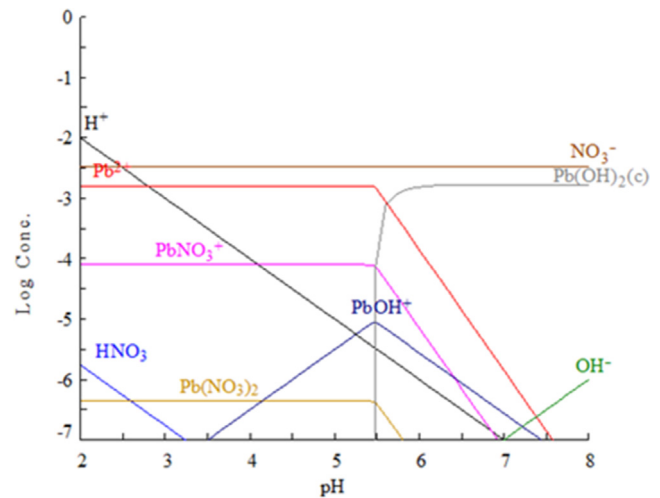


**Fig. 5** Lead species distribution diagram calculated for the experimental conditions used in this work.

negatively-charged surface groups might be expected. However, the extent of the reactions forming these surface groups might be limited due to the small gradient between the initial solution pH and the IIP of samples SB, SC and SD.

In the other hand, a lead species distribution diagram was calculated by using Medusa software (Puigdomenech, 2010) under the same conditions used for the experimental work: initial Pb(II) concentration = 538 mg/L, 1 atm and 25 °C. The lead species distribution diagram shown in Fig. 5 indicates that at pH = 5 the most stable lead species is Pb(II) ion. This cation could be adsorbed by electrostatic attraction if enough negatively-charged surface groups such as FeO<sup>-</sup> exist on the BFD samples. In this scenario, Pb(II) adsorption may be related to the number of surface FeOH<sup>-</sup> groups formed when the BFD samples is immersed in aqueous solution. However, the small differences in the pH<sub>IIP</sub> observed from the BFD samples suggested that the number of potential surface FeOH<sup>-</sup> groups available for Pb(II) adsorption was about the same. As a result, the differences in Q<sub>e</sub> observed for the various BFD samples could not be explained by Pb(II) adsorption, thus suggesting that other surface process must be taking place in parallel to promote Pb(II) removal, as a function of the chemical composition of the samples.

It should be noticed that Fig. 4d) showed that Pb adsorption decreased with the Fe<sub>2</sub>O<sub>3</sub> and Fe<sub>3</sub>O<sub>4</sub> content. This observation suggested that equations (8), 10 and 12 were favoured because pH was acid (i.e. pH < pH<sub>IIP</sub>) and, as a result, [H<sup>+</sup>] > [OH<sup>-</sup>]. On the other hand, Fig. 4c) showed that the amount of adsorbed Pb increased with the Fe<sup>0</sup> and FeO content. Due to the fact that the standard reduction potential of Fe<sup>2+</sup>/Fe<sup>0</sup> is -0.44 V, which is lower than that of Pb<sup>2+</sup>/Pb (-0.13 V), then lead ions could react with metallic iron as an electron donor and precipitate (Rezaei and Vione, 2018), following reduction into insoluble metal forms, according to the following reaction:



In the case of FeO, Pb could be removed by ion exchange, like CaO, in agreement with the following reaction:

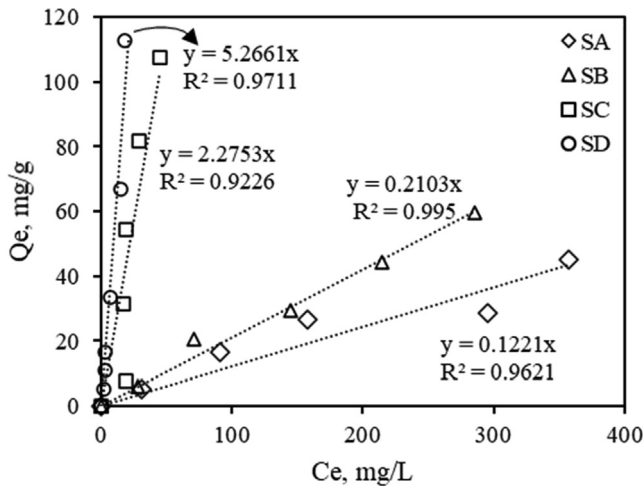
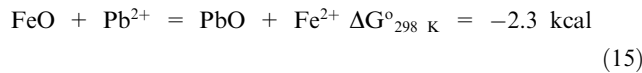
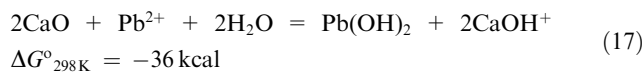
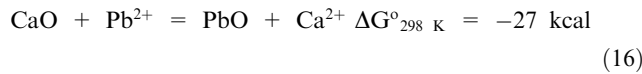


**Fig. 6** Comparison of Pb(II) adsorption experimental data with predictions from Henry's adsorption isotherm for SA, SB, SC and SD samples.



In the other hand, as it is shown in [Table 4](#) and [Fig. 4a](#)),  $Q_e$  was clearly a function of CaO + MgO content in BFD samples. This trend was in agreement with the recent reports in the literature. In fact, [Zhan et al. \(2019\)](#) reported that in solutions with  $\text{pH} < 7$ ,  $\text{Pb}^{2+}$  can be adsorbed by ion exchange with Ca ions, resulting of the hydrolysis of CaO (or calcium and magnesium aluminosilicates) contained in the samples. It should be pointed out that in this study the solution pH could have slightly increased by the alkaline nature of BFD samples. According to the lead distribution diagram shown in [Fig. 6](#), for pH above 5.5 Pb could have been hydrolysed in the form of  $\text{Pb}(\text{OH})^+$  and  $\text{Pb}(\text{OH})_2$ . Based on these premises, a feasible mechanism of Pb(II) removal under the conditions of this study could be started by  $\text{Pb}(\text{OH})^+$  adsorption, followed by complexation to  $\text{Pb}(\text{OH})_2$ , and  $\text{Pb}(\text{OH})_2$  precipitation. In the other hand, it may be suggested that  $\text{Pb}^{2+}$  could be removed from the aqueous solution by an ion exchange process according to the following reactions (Gibbs energy obtained from HSC 6.1 software ([Roine, 2006](#))):



Similar reactions may also occur for MgO. However, taking in consideration the larger composition of CaO with respect to MgO in the BFD samples, CaO was considered as the most important contribution.

Taking into account the change in Gibbs free energy for the chemical reactions occurring in the system and the composition of CaO, Fe and FeO in BFD samples, it could be postulated that the removal of Pb(II) from aqueous solution, under the conditions used in this study, may include two routes: i) Pb (II) is removed by ion exchange with CaO and MgO, ii) Pb(II) is removed by precipitation on the surface of iron phases.

These two routes may be occurring to different extent in parallel mode. The predominance or extent of each Pb(II) removal processes is determined by the change in Gibbs free energy of the surface reactions (14) to (17), as also by the relative composition of basic oxides (CaO and MgO) and two of the iron species (Fe and FeO) in the BFD samples. Thus, the removal of Pb(II) from aqueous solutions is a strong function of the chemical composition of BFD samples; in fact, it is mostly enhanced by the content of CaO and MgO through an ion exchange process, and by Fe and FeO species through a precipitation process.

### 3.3. Adsorption isotherm analysis

Henry, Langmuir, Freundlich, Tempkin and Dubinin-Radushkevich adsorption isotherm models have been used to describe the adsorption process ([Limousin et al., 2007](#); [Ayawei et al., 2017](#)). Henry's isotherm is the simplest adsorption isotherm model, and it represents the thermodynamic adsorption limit at low surface coverage, assuming that there is no interaction among the adsorbed molecules ([Silva da Rocha et al., 1998](#)). In agreement with Henry's model,  $Q_e$  is proportional to the  $C_e$ :

$$Q_e = K_H C_e \quad (18)$$

where  $K_H$  is Henry's adsorption constant.

In the other hand, Langmuir isotherm model assumes that adsorbate molecules adsorb with uniform energy on the adsorbent external surface, progressively filling the available adsorption sites; the limiting adsorption condition is the formation of a monolayer of adsorbed molecules ([Ayawei et al., 2017](#)). In this model,  $Q_e$  is a function of  $C_e$  as given by the following equation ([Al-Ghouti and Da'ana, 2020](#)).

$$Q_e = \frac{Q_{\max} K_L C_e}{1 + K_L C_e} \quad (19)$$

Where  $Q_{\max}$  is the maximum monolayer coverage capacity (mg/g), and  $K_L$  is the Langmuir isotherm constant (L/mg).

The empirical Freundlich adsorption model is generally used to describe adsorption process on heterogeneous surfaces, according to the following equation ([Ezzati, 2020](#)):

$$Q_e = K_f C_e^{1/n} \quad (21)$$

Where  $K_f$  is the Freundlich isotherm constant ((mg/g)(L/mg)<sup>1/n</sup>), which is an indicator of adsorption capacity and  $n$  is the adsorption intensity parameter; in fact,  $1/n$  is a function of the strength of the adsorption process ([Fang et al., 2020](#)).

In the other hand, Tempkin's adsorption model assumes that heat of adsorption would decrease linearly with surface coverage ([Aharoni and Ungarish, 1997](#)) and it includes a factor that explicitly considers the adsorbent-adsorbate interactions:

$$Q_e = \frac{RT}{b} \ln(A_T C_e) \quad (22)$$

where:  $A_T$  is the Tempkin isotherm equilibrium binding constant (L/g),  $b$  is the Tempkin isotherm constant,  $T$  is the adsorption temperature,  $R$  is the universal gas constant; the factor  $B = RT/b$ , is a constant related to heat of sorption (J/mol).

Finally, Dubinin-Radushkevich isotherm model has been successfully used to fit high solute activities and the intermediate range of concentration data ([Hutson and Yang, 1997](#); [Hu and Zhang, 2019](#)).

**Table 6** Pb(II) adsorption isotherm parameters for SA, SB, CD, SD samples.

Isotherm model	Parameter	Samples			
		SA	SB	SC	SD
Henry	$r^2$	0.962	0.995	0.923	0.971
	$K_H$	0.1221	0.2103	2.2753	5.2661
Freundlich	$r^2$	0.975	0.943	0.850	0.985
	$n$	1.062	1.255	0.887	0.833
	$K_f$	0.293	0.395	1.589	2.994
Langmuir	$r^2$	0.943	0.99	0.777	0.974
	$Q_0$	105	137	222	147
	$K_L$	$3 \times 10^{-3}$	$3 \times 10^{-3}$	$-8 \times 10^{-3}$	$-2 \times 10^{-2}$
	$R_L$	0.496	0.498	0.511	0.532
Tempkin	$r^2$	0.917	0.878	0.950	0.874
	$A$	$1 \times 10^{-4}$	$1 \times 10^{-3}$	$3 \times 10^{-4}$	$1 \times 10^{-3}$
	$bt$	116	176	33	50
	$B$	21.3	14	74.6	49.8
Dubinin-Radushkevich	$r^2$	0.766	0.878	0.922	0.938
	$K_{ad}$	$8 \times 10^{-4}$	$3 \times 10^{-4}$	$6 \times 10^{-5}$	$4 \times 10^{-6}$
	$qs$	49.58	30.08	133.77	77.51
	$E$	0.025	0.042	0.085	0.341

$$Qe = (qs)\exp(-K_{ad}\varepsilon^2) \quad (23)$$

where:  $qs$  is a theoretical isotherm saturation capacity (mg/g),  $K_{ad}$  is the Dubinin–Radushkevich isotherm constant ( $\text{mol}^2/\text{kJ}^2$ ) and  $\varepsilon$  is the adsorption potential.

The indicated adsorption models were used to fit the experimental adsorption data of Pb (II) removal from aqueous solutions by using BFD samples. The set of parameters that better fitted the experimental data to each adsorption model was summarized in Table 6, which also includes the correlation coefficient ratio ( $r^2$ ) as the error function to determine the best-fitting relationship (Foo and Hameed, 2010). Henry's isotherm model showed the best linear fit for SA, SB and SD, with  $r^2 > 0.96$ . Only SC had a slightly lower  $r^2$  value. Fig. 6 shows the agreement between experimental data and the predictions of the Henry's adsorption model.  $K_H$  values varied for BFD samples in the following order  $SD > SC \gg SB > SA$ , thus resembling the same order experimentally observed for Pb(II) adsorption capacity ( $Q_e$ ).

Langmuir isotherm model also made a reasonable fit of the experimental adsorption data for SA, SB and SD, showing  $r^2 > 0.94$ . In the other hand, Freundlich adsorption model was less adequate than Henry's and Langmuir's adsorption models to fit the experimental data ( $r^2 > 0.85$ ). However, Freundlich's adsorption parameters,  $K_f$  and  $1/n$ , related to the adsorption capacity and to the strength of the adsorption process (Foo and Hameed, 2010), respectively, clearly showed that the Pb(II) adsorption was more favourable in SC and SD. Based on the fitting of Tempkin's adsorption,  $B$  constant value for SD and SC was at least twice the  $B$  values for SA and SB, suggesting stronger interactions between the adsorbate and the surface. Finally, Dubinin–Radushkevich adsorption model showed that constant  $q_s$ , related to heat of adsorption, varied in the following order:  $SC \gg SD > SA > SB$ , while the free energy  $E$  values varied in the order  $SD \gg SC > SB > SA$ . These trends suggested that Pb(II) removal could be related to the ion exchange processes described in the previous sec-

tions. In brief, the best fit of equilibrium adsorption data for all BFD samples was obtained by using Henry's adsorption model. Complementary, the other adsorption models also described the higher adsorption capacity of SC and SD, and they provided the basis to support that Pb(II) adsorption by ion exchange (mainly due to the CaO content and favoured by a smaller particle size) may be a predominant mechanism in the BFD samples used in this study.

### 3.4. Kinetics analysis of Pb(II) removal

Kinetics of Pb(II) removal process was studied by using SC. As it was indicated SC comes from a single equipment (wet scrubber), so it would have better traceability for quality purposes and, its addition, it displayed a large  $Q_e$ . Kinetic studies of Pb(II) removal were conducted at atmospheric pressure, 25 °C and using an aqueous solution with initial Pb(II) concentration of 120 mg/L. Fig. 7a showed that Pb(II) concentration in the aqueous solution continuously decreased as a function of contact time. The fastest Pb(II) removal took place over the first 5 min. A Pb(II) removal of about 90% was reached after 20 min. The fast adsorption of Pb(II) observed at short contact times may be attributed to external surface reactions, such as ion exchange or precipitation reactions, suggested in this study as the most feasible Pb(II) removal mechanisms. In this way, Pb(II) ions could easily reach active sites due to a relatively high CaO and Fe and FeO surface concentration, thus resulting in a rapid Pb(II) uptake. As the reaction progressed, the rate of Pb(II) removal decreased as the availability of Ca and Fe surface species suitable for the surface reactions processes became scarce and Pb(II) ions must diffuse through the sample pores to find new active sites.

Data of the kinetic experiment were fitted by models typically used to describe transient metal removal processes (Fulbert, 2019; Wang and Guo, 2020). A pseudo-first order kinetic model, based on the Lagergren equation, was initially used:

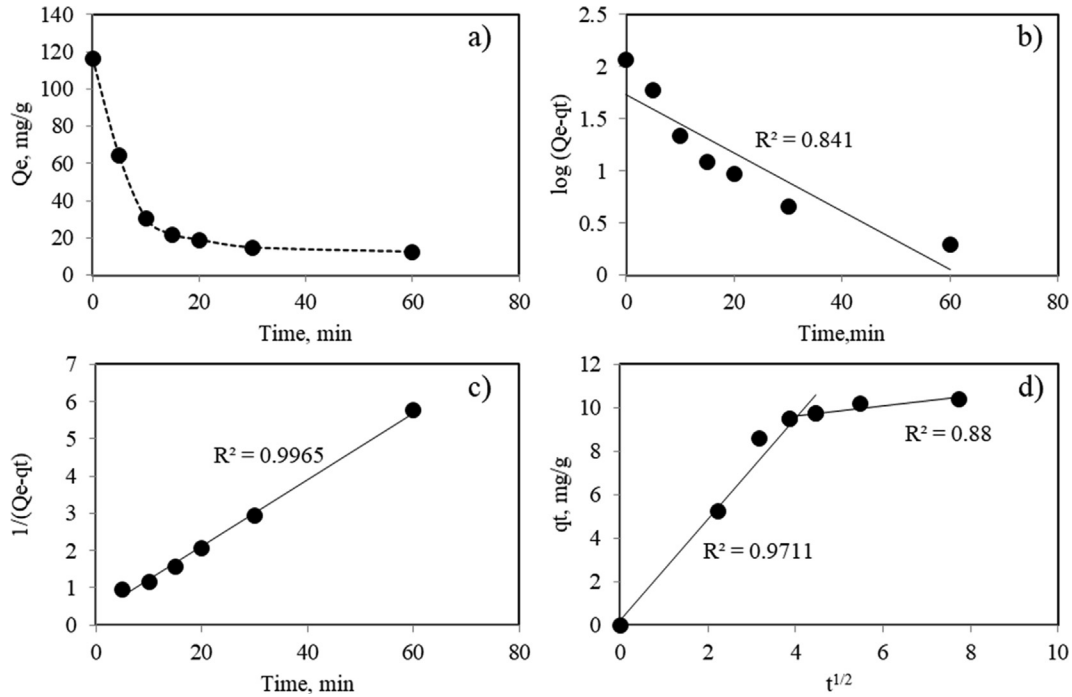


**Fig. 7** a) Pb(II) removal by sample SC under dynamic conditions (1 g BDF in 100 mL solution with initial Pb(II) concentration = 538 mg/L, pH = 5 and 25 °C). Fit of experimental data by using: b) Pseudo-first order kinetic model, c) Pseudo-second order kinetic model, d) Intraparticle diffusion model.

$$\frac{dQ}{dt} = k_1(Q_e - Q_t) \quad (24)$$

where  $Q_t$  and  $Q_e$  (mg/g) are the amount of solute adsorbed at time  $t$  (min) and at equilibrium, respectively, and  $k_1$  ( $\text{min}^{-1}$ ) is a first order rate constant.

A pseudo-second order kinetic model, which is described by the following equation, was also used:

$$\frac{dQ}{dt} = k_2(Q_e - Q_t)^2 \quad (25)$$

where the driving force ( $Q_e - Q_t$ ) is proportional to the available fraction of active sites and  $k_2$  is the second order rate constant (Kaushal and Singh, 2017).

Finally, an intraparticle diffusion model was also used to fit the experimental data. This model assumes that adsorption rate is controlled by internal or intraparticle diffusion of Pb(II) ions in the sample, the governing rate of Pb(II) removal is given by the following equation (Li et al., 2013):

$$q_t = k_{id}t^{1/2} \quad (26)$$

where  $k_{id}$  is the intraparticle diffusion rate constant. In this way, a linear fit of the plot of  $q_t$  vs  $t^{1/2}$  is representative of an intraparticle diffusion adsorption process. The slope yields the intraparticle diffusion rate constant  $k_{id}$  and the intercepts reflects the boundary layer (BL) effect.

Results of the fitting of the experimental data with the kinetic models previously described and kinetics parameters were summarized in Fig. 7 and Table 7, respectively.

Clearly, the pseudo first order kinetic model did not fit the kinetic data ( $r^2 = 0.841$ ). Similarly, the intraparticle diffusion model was not able to correlate the experimental data. Finally, the pseudo-second-order model showed a good fit of the kinetic data ( $r^2 = 0.9926$ ) and it was assumed as the best

**Table 7** Kinetic parameters values determined by fitting of experimental data of Pb(II) removal under dynamic conditions for sample SC.

Kinetic model	Parameters			$r^2$
a) Pseudo-1st order	$Q_e$	$K_{ad}$		0.841
	53.33	0.064		
b) Pseudo-2nd order	$Q_e$	$K_2$	$h$	0.996
	11.15	0.025	3.159	
c) Intraparticle diffusion	BL effect	$K_{id}$		0.989
	0.24	2.32		

model to describe the transient Pb(II) removal process. This finding may support that Pb(II) removal occur through bimolecular reactions such as ion exchange or the precipitation of Pb(II) with either CaO or Fe species, respectively.

### 3.5. Practical implications of using BFD for removal of Pb(II) ions in aqueous solutions

Results in previous sections clearly showed that it is possible to use BFD samples, collected from a dust collector system installed in a steelmaking plant, to remove Pb(II) from aqueous solutions at 25 °C and initial pH = 5.0. Results of this study confirm that chemical composition of BFD samples play a key role for Pb(II) removal. In more detailed, both CaO and MgO content in BFD samples had a positive linear correlation with Pb removal and  $Q_e$ . As suggested by Zhang et al. [18], it was shown that removal of Pb(II) may occur through an ion exchange process with Ca ions. The analysis suggested that

removal of Pb(II) by MgO followed a similar mechanism; however, MgO promoted the Pb(II) removal in lesser extent because it is less thermodynamic favourable and because its composition is 10 times lower than CaO. In a similar way, it was shown that iron species had a promotional effect for Pb(II) removal from aqueous solutions. It was evident that less oxidized iron species (i.e., Fe<sup>0</sup> and FeO) favoured Pb(II) removal. Under the conditions used in this study, it was postulated that iron species remove Pb through an ion exchange process. The beneficial effect of Fe species was explained in terms of a lower change of Gibbs free energy, being the of the exchange process with Fe more favourable than FeO. These bimolecular ion exchange process between Pb(II) ions and Ca and Fe species was further supported by results obtained from equilibrium and transient adsorption process.

The Pb(II) removal performance of the samples collected from a dust collector system of in a steelmaking plant showed that those residues collected at the end of the collector system, SC (from the wet scrubber) and SD (from the sludge dam) exhibited higher Pb(II) adsorption capacity, 107.6 and 112.8 mg/g, respectively. This range of Pb(II) adsorption capacity of these BFD samples is similar to  $Q_e$  values reported in the literature for analogous residues (furnace sludge and ladle furnace steel dust). It is noteworthy that the BFD samples used in this study were not subjected to any pre-treatment and, therefore, must be taken as a residue of the steelmaking process that can be directly valorised for the removal of heavy metals such as Pb(II) ions, with potential economic benefits in the treatment of polluted industrial effluents. Finally, based on the results of this study, a set of guidelines could be set to improve the Pb(II) adsorption capacity of the BFD samples. However, these improvements, such as the tuning of the particle size, the adjustment of T and initial pH, or the chemical treatment of the BFD, may have economic implications for the practical viability of the heavy metal removal process.

#### 4. Conclusions

In the context of circular economy, the re-use of metallurgical wastes has an increasing relevance, and a number of innovative applications are under development. One of the most promising applications is water treatment of industrial effluents due to its high availability, low cost, high chemical affinity for heavy metals and magnetic properties that facilitate their recovery after treatment. Several studies have addressed the effect of experimental conditions on the removal of heavy metals such as lead from aqueous solutions. This study focused on the effect of chemical composition of steelmaking residues on the maximum Pb(II) adsorption capacity ( $Q_e$ ) from synthetic aqueous solutions, by using samples collected from different sections of a dust collector system in a steelmaking factory. Chemical composition of the BFD samples used in the study showed the presence of iron species (Fe, FeO, Fe<sub>2</sub>O<sub>3</sub> and Fe<sub>3</sub>O<sub>4</sub>), basic oxides (CaO, MgO, SiO<sub>2</sub>) and C species as the main components. Equilibrium and transient experiments of Pb(II) removal from aqueous solutions by BFD samples were conducted at 25 °C and initial pH = 5.0. Results showed that CaO and MgO, as well as metallic Fe and FeO had a positive linear effect in Pb(II) removal and  $Q_e$ . Under the experimental conditions used in this study, Pb(II) removal process may take

place by two parallel routes; Pb(II) is removed by ion exchange with CaO and MgO, and Pb(II) is also removed by precipitation on the surface of iron phases. A thermodynamics analysis of the surface chemistry suggested that MgO and FeO promoted the Pb(II) removal in lesser extent than CaO and metallic Fe, respectively, because the surface ion exchange with MgO and FeO are less thermodynamic favourable and their lower composition in the sample. These bimolecular ion exchange process between Pb(II) ions and Ca and Fe species was further supported by results obtained from equilibrium and transient adsorption process. Results of this work clearly showed that removal of Pb(II) from aqueous solutions is a strong function of the chemical composition of BFD samples and it provided further insight to promote the valorisation of steelmaking residues as heavy-metal adsorbents, contributing to future development of sustainable processes.

#### Declaration of Competing Interest

Authors declare no conflicts of interest.

#### Acknowledgements

Authors thank the International Center for Nanotechnology and Advanced Materials - Kleberg Advanced Microscopy Center - at the University of Texas at San Antonio (ICNAM-UTSA) for technical characterization assistance.

#### References

- Aharoni, C., Ungarish, M., 1997. Kinetics of activated chemisorptions. Part 2 Theoretical models. *J. Chem. Soc. Faraday Trans. 1*, 73, 456–464. <https://doi.org/10.1039/F19777300456>.
- Al-Asheh, S., Banat, F., Al-Omari, R., Duvnjak, Z., 2000. Predictions of Binary Sorption Isotherms for the Sorption of Heavy Metals by Pine Bark Using Single Isotherm Data. *Chemosphere* 41 (5), 659–665. [https://doi.org/10.1016/S0045-6535\(99\)00497-X](https://doi.org/10.1016/S0045-6535(99)00497-X).
- Alghamdi, A., Al-Odayni, A., Saeed, W., Al-Kahtani, A., Alharthi, F., Aouak, T., 2019. Efficient adsorption of lead (ii) from aqueous phase solutions using polypyrrole-based activated carbon. *Materials* 12, 12. <https://doi.org/10.3390/ma12122020>.
- Al-Ghouti, M., Da'ana, D., 2020. Guidelines for the use and interpretation of adsorption isotherm models: A review. *J. Hazardous Mater.* 393, 122383. <https://doi.org/10.1016/j.jhazmat.2020.122383>.
- Andersson, A., Ahmed, H., Rosenkranz, J., Samuelsson, C., Björkman, B., 2017. Characterization and upgrading of a low zinc-containing and fine blast furnace sludge – a multi-objective analysis. *ISIJ Int.* 57 (2), 262. <https://doi.org/10.2355/isijinternational.ISIJINT-2016-512>.
- Arbabi, M., Hemati, S., Amiri, M., 2015. Removal of lead ions from industrial wastewater: A review of removal methods. *Int. J. Epidemiologic Res.* 2 (22), 105–109.
- Asuero, A., Sayago, A., Gonzalez, A., 2006. The Correlation Coefficient: An Overview. *Crit. Rev. Anal. Chem.* 36, 41–59. <https://doi.org/10.1080/10408340500526766>.
- Ata, S., Tabassum, A., Bibi, I., Majid, F., Sultan, M., Ghafoor, S., Bhatti, M., Qureshi, N., Iqbal, M., 2018. Lead remediation using smart materials. A review. *Zeitschrift für Physikalische Chem.* 223, 10. <https://doi.org/10.1515/zpch-2018-1205>.
- Ayawei, N., Ebelegi, A., Wankasi, D., 2017. Modelling and Interpretation of Adsorption Isotherms. *J. Chem.* 2017. <https://doi.org/10.1155/2017/3039817>.
- Bădescu, S., Bulgariu, D., Ahmad, I., Bulgariu, L., 2018. Valorisation possibilities of exhausted biosorbents loaded with metal ions - A

- review. *J. Environ. Manag.* 224, 288–297. <https://doi.org/10.1016/j.jenvman.2018.07.066>.
- Bhatnagar, A., Jain, A., 2006. Removal of Lead Ions from Aqueous Solutions by Different Types of Industrial Waste Materials: Equilibrium and Kinetic Studies. *Sep. Sci. Technol.* 41, 1881–1892. <https://doi.org/10.1080/01496390600725828>.
- Bouabidi, Z., El-Naas, M., Cortes, D., McKay, G., 2018. Steel-making dust as a potential adsorbent for the removal of lead (II) from an aqueous solution. *Chem. Eng. J.* 334, 837–844. <https://doi.org/10.1016/j.cej.2017.10.073>.
- Boslaugh, S., Watters, P., 2008. *Statistics in a Nutshell: A Desktop Quick Reference*, ch. 7. Sebastopol, CA: O'Reilly Media. ISBN-13: 978-0596510497.
- Chung, N., Hanh, T., Nguyen, T., 2016. Adsorptive removal of five heavy metals from water using blast furnace slag and fly ash. *J. Sci. Technol.* 54, 314–320. <https://doi.org/10.1007/s11356-017-9610-4>.
- Cooney, D.O., 1998. *Adsorption Design for Wastewater Treatment*, CRC Press, ISBN 9781566703338.
- Ezzati, R., 2020. Derivation of Pseudo-First-Order, Pseudo-Second-Order and Modified Pseudo-First-Order rate equations from Langmuir and Freundlich isotherms for adsorption. *Chem. Eng. J.* 392, 123705. <https://doi.org/10.1016/j.cej.2019.123705>.
- Fang, D., Zhuang, X., Huang, L., Zhang, Q., Shen, Q., Jiang, L., Xu, X., Ji, F., 2020. Developing the new kinetics model based on the adsorption process: From fitting to comparison and prediction. *Sci. Total Env.* 725, 138490. <https://doi.org/10.1016/j.scitotenv.2020.138490>.
- Fisher, L.V., Barron, A.R., 2019. The recycling and reuse of steelmaking slags — A review. *Resources. Conserv. Recycl.* 146, 244–255. <https://doi.org/10.1016/j.resconrec.2019.03.010>.
- Foo, K., Hameed, B., 2010. Insights into the modelling of adsorption isotherm systems. *Chem. Eng. J.* 156 (1), 2–10. <https://doi.org/10.1016/j.cej.2009.09.013>.
- Fulbert, T., 2019. Modelling adsorption mechanism of paraquat onto Ayous (*Triplochiton scleroxylon*) wood sawdust. *Appl. Water Sci.* 9, 1. <https://doi.org/10.1007/s13201-018-0879-3>.
- Ghaedi, M., Mosallanejad, N., 2013. Removal of heavy metal ions from polluted waters by using of low-cost adsorbents: Review. *J. Chem. Health Risk* 3 (1), 07–22. <https://dx.doi.org/10.22034/jchr.2018.544016>.
- Hosseinzadeh, M., Ebrahimi, S., Raygan, S., Masoudpanah, S., 2016. Removal of cadmium and lead ions from aqueous solution by nanocrystalline magnetite through mechanochemical activation. *J. Ultrafine Grained Nanostruct. Mater.* 49 (2), 72–79. 10.7508.jufgsm/2016.02.03.
- Hu, Q., Zhang, Z., 2019. Application of Dubinin-Radushkevich isotherm model at the solid/solution interface: A theoretical analysis. *J. Mol. Liq.* 277 (1), 646–648. <https://doi.org/10.1016/j.molliq.2019.01.005>.
- Huy, D., Seelen, E., Liem-Nguyen, V., 2020. Removal mechanisms of cadmium and lead ions in contaminated water by stainless steel slag obtained from scrap metal recycling. *J. Water Process Eng.* 36, 101369. <https://doi.org/10.1016/j.jwpe.2020.101369>.
- Hutson, N., Yang, R., 1997. Theoretical basis for the Dubinin-Radushkevich (D-R) adsorption isotherm equation. *Adsorption* 3 (3), 189–195. <https://doi.org/10.1007/BF01650130>.
- Jalkanen, H., Oghbasilasie, H., Raipala, K., 2005. Recycling of steelmaking dusts – the radust concept. *J. Mining Metall.* 41, 1–16. <https://doi.org/10.2298/JMMB0501001J>.
- Juned, M., Ahmed, K., Ahmaruzzaman, M., 2016. A review on potential usage of industrial waste materials for binding heavy metal ions from aqueous solutions. *J. Water Process Eng.* 10, 39–47. <https://doi.org/10.1016/j.jwpe.2016.01.014>.
- Kaushal, A., Singh, S., 2017. Adsorption phenomenon and its application in removal of lead from wastewater: a review. *Int. J. Hydro.* 1 (2), 38–47. <https://doi.org/10.15406/ijh.2017.01.00008>.
- Kennedy, A.M., Arias-Paić, M., 2020. Application of powdered steel slag for more sustainable removal of metals from impaired waters. *J. Water Process Eng.* 38, <https://doi.org/10.1016/j.jwpe.2020.101599> 101599.
- Kim, S.H., Chung, H., Jeong, S., Nam, K., 2021. Identification of pH-dependent removal mechanisms of lead and arsenic by basic oxygen furnace slag: Relative contribution of precipitation and adsorption. *J. Clean. Prod.* 279, 123451. <https://doi.org/10.1016/j.jclepro.2020.123451>.
- Kosmulski, M., 2020. The pH dependent surface charging and points of zero charge. *Adv. Colloid Interface Sci.* 275, 1–18. <https://doi.org/10.1016/j.cis.2019.102064>.
- Li, L., Fan, L., Sun, M., Qiu, H., Li, X., Duan, H., Luo, C., 2013. Adsorbent for lead removal based on graphene oxide functionalized with magnetic cyclodextrin–chitosan. *Coll. Surf. B Biointerf.* 107, 76–83. <https://doi.org/10.1016/j.colsurfb.2013.01.074>.
- Limousin, G., Gaudet, J.P., Charlet, L., Szenknect, S., Barthès, V., Krimissa, M., 2007. Sorption isotherms: A review on physical bases, modeling and measurement. *Appl. Geochem.* 22 (2), 249–275. <https://doi.org/10.1016/j.apgeochem.2006.09.010>.
- Liu, S., Gao, J., Yang, Y., Yang, Y., Ye, X., 2010. Adsorption intrinsic kinetics and isotherms of lead ions on steel slag. *J. Hazard. Mater.* 173 (1–3), 558–562. <https://doi.org/10.1016/j.jhazmat.2009.08.122>.
- Lopez-Delgado, A., Perez, C., Lopez, F., 1998. Sorption of heavy metals on blast furnace sludge. *Wat. Res.* 32 (4), 989–996. [https://doi.org/10.1016/S0043-1354\(97\)00304-7](https://doi.org/10.1016/S0043-1354(97)00304-7).
- Lucaci, A., Dimbu, R., Bulgariu, D., Bulgariu, L., 2019. Use of Iron Nanoparticles Functionalized with Alginate for the Adsorption of Pb(II) Ions from Aqueous Media. 2019 E-Health and Bioengineering Conference (EHB), Iasi, Romania, 1–4, <https://doi.org/10.1109/EHB47216.2019.8969913>.
- Mercado-Borrayo, B., Contreras, R., Sánchez, A., Font, X., Schouwe-naars, R., Ramírez-Zamora, R., 2020. Optimisation of the removal conditions for heavy metals from water: A comparison between steel furnace slag and CeO<sub>2</sub> nanoparticles. *Arabian J. Chem.* 13 (1), 1712–1719. <https://doi.org/10.1016/j.arabjc.2018.01.008>.
- Nilforoushan, M.R., Otroj, S., 2008. Adsorption of Lead Ions by Various Types of Steel Slag. *Iran. J. Chem. Chem. Eng.* 27 (3), 69–75. [http://www.ijcce.ac.ir/article\\_6969\\_49d1e0b2e7485ff3ccb95591f52587a4.pdf](http://www.ijcce.ac.ir/article_6969_49d1e0b2e7485ff3ccb95591f52587a4.pdf).
- Naidu, T.S., Sheridan, C.-M., van Dyk, L.D., 2020. Basic oxygen furnace slag: Review of current and potential uses. *Minerals Eng.* 149, 106234. <https://doi.org/10.1016/j.mineng.2020.106234>.
- Nassar, N.N., 2010. Rapid removal and recovery of Pb(II) from wastewater by magnetic nanoadsorbents. *J. Hazardous Mater.* 184 (1–3), 538–546. <https://doi.org/10.1016/j.jhazmat.2010.08.069>.
- Olowoyo, D., Garuba, A., 2012. Adsorption of cadmium ions using activated carbon prepared from Coconut shell. *Global Adv. Res. J. Food Sci. Technol.* 1 (6), 81–84.
- Panamerican Health Organization Site, [https://www.paho.org/hq/index.php?option=com\\_content&view=article&id=8206:2013-lead-contamination&Itemid=39800&lang=en](https://www.paho.org/hq/index.php?option=com_content&view=article&id=8206:2013-lead-contamination&Itemid=39800&lang=en) (accessed July 2020).
- Puigdomenech, I., 2010. MEDUSA Software, Royal Institute of Technology, Stockholm, Sweden.
- Rezaei, F., Vione, D., 2018. Effect of pH on zero valent iron performance in heterogeneous Fenton and Fenton-Like processes: A review. *Molecules* 23, 31–127. <https://doi.org/10.3390/molecules23123127>.
- Roine, A., 2006. HSC Chemistry 6.0, Outotec Research Oy, Pori, Finland.
- Roy, A., Bhattacharya, J., 2012. Removal of Cu (II), Zn (II) and Pb (II) from water using microwave-assisted synthesized maghemite nanotubes. *Chem. Eng. J.* 211, 493–500. <https://doi.org/10.1016/j.cej.2012.09.097>.
- Sarkar, S., Mazumder, D., 2015. Solid waste management in steel industry - challenges and opportunities. *Int. J. Social, Behav. Educ. Econ., Bus. Ind. Eng.* 9 (3), 978–981. [https://doi.org/10.1007/978-981-13-7071-7\\_27](https://doi.org/10.1007/978-981-13-7071-7_27).

- Soliman, N.K., Moustafa, A.F., 2020. Industrial solid waste for heavy metals adsorption features and challenges; a review. *J. Mater. Res. Technol.* 9 (5), 10235–10253. <https://doi.org/10.1016/j.jmrt.2020.07.045>.
- Silva da Rocha, M., Antonio, K., Faleiros, C., Corat, E., Vázquez Suárez-Iha, M., 1998. Henry's Law as a Limit for an Isotherm Model Based on a Statistical Mechanics Approach. *J. Colloid Interface Sci.* 208 (1), 211–215. <https://doi.org/10.1006/jcis.1998.5779>.
- Srivastava, S., Gupta, V., Mohan, D., 1997. Removal of lead and chromium by activated slag-a blast-furnace waste. *J. Environ. Eng.* 123, 461–468. [https://doi.org/10.1061/\(ASCE\)0733-9372\(1997\)123:5\(461\)](https://doi.org/10.1061/(ASCE)0733-9372(1997)123:5(461)).
- Ugwu, I.M., Igbokwe, O.A., 2019. Sorption of Heavy Metals on Clay Minerals and Oxides: A Review. *Advanced Sorption Process Applications*, Serpil Edebalı, IntechOpen. <https://doi.org/10.5772/intechopen.80989>.
- Vijayakumar, S., Sasikala, M., Ramesh, R., 2012. Lead poisoning – An overview. *Int. J. Pharmacol. Toxicol.* 2 (2), 70–82.
- Vu, H., Gu, S., Thriveni, T., Khan, M., Tuan, L., Ahn, J., 2019. Sustainable treatment for sulfate and lead removal from battery wastewater. *Sustainability* 11, 3497. <https://doi.org/10.3390/su11133497>.
- Vu, M.T., Nguyen, L.N., Johir, M.A.H., Ngo, H.H., Skidmore, C., Fontana, A., Galway, B., Bustamante, H., Nghiem, L.D., 2021. Phosphorus removal from aqueous solution by steel making slag – Mechanisms and performance optimisation. *J. Cleaner Prod.* 284, 124753. <https://doi.org/10.1016/j.jclepro.2020.124753>.
- Wang, J., Guo, X., 2020. Adsorption kinetic models: Physical meanings, applications, and solving methods. *J. Hazard. Mater.* 390, 122156. <https://doi.org/10.1016/j.jhazmat.2020.122156>.
- WHO Guidelines for Drinking-water Quality, [https://www.who.int/water\\_sanitation\\_health/dwq/chemicals/lead.pdf](https://www.who.int/water_sanitation_health/dwq/chemicals/lead.pdf) (accessed July 2020).
- Xiong, C., Wang, W., Tan, F., Luo, F., Chen, J., Qiao, X., 2015. Investigation on the efficiency and mechanism of Cd (II) and Pb (II) removal from aqueous solutions using MgO nanoparticles. *J. Hazard. Mater.* 299, 664–674. <https://doi.org/10.1016/j.jhazmat.2015.08.008>.
- Yiacoumi, S., Tien, C., 1995. *Kinetics of Metal Ion Adsorption from Aqueous Solutions: Models, Algorithms, and Applications*. Springer, US. ISBN 978-1-4615-2319-2.
- Yang, L., Wen, T., Wang, L., Miki, T., Bai, H., Lu, X., Yu, H., Nagasaka, T., 2019. The stability of the compounds formed in the process of removal Pb(II), Cu(II) and Cd(II) by steelmaking slag in an acidic aqueous solution. *J. Environ. Manage.* 231, 41–48.
- Zahra, N., Pak, J., 2012. Lead removal from water by low cost adsorbents: A review. *Anal. Environ. Chem.* 13, 1–8.
- Zhan, X., Xiao, L., Liang, B., 2019. Removal of Pb(II) from Acid Mine Drainage with Bentonite-Steel Slag Composite Particles. *Sustainability* 11, 4476. <https://doi.org/10.3390/su11164476>.
- Zhu, Y., Hu, J., Wang, J., 2012. Competitive adsorption of Pb (II), Cu (II) and Zn (II) onto xanthate-modified magnetic chitosan. *J. Hazard. Mater.* 221, 155–161. <https://doi.org/10.1016/j.jhazmat.2012.04.026>.